ELSEVIER

Ceramics International 26 (2000) 685–692

CERAMICS
INTERNATIONAL

# Microstructural evolution in $MSnO_3$ ceramics derived via self-heat-sustained (SHS) reaction technique

Abdul-Majeed Azad *, Lucia Liew Woan Shyan, Toh Yen Pang, Chen Hon Nee

*Department of Physics, University Putra Malaysia, 43400 UPM Serdang, Selangor, Malaysia*

Received 20 September 1999; received in revised form 9 October 1999; accepted 23 November 1999

**Abstract**

A thorough study of $MSnO_3$ (M = Ca, Sr and Ba) compounds with respect to their synthesis, processing and microstructural characterization has been made. In order to establish a standard methodology with identical and beneficial microstructure and reproducible electrical characteristics, a novel preparative method called self-heat-sustained (SHS) reaction technique was employed. Evolution of microstructure which is intimately related to the envisaged properties in the ceramics, was closely and systematically followed in terms of wide temperature-soak time (*T-t*) profiles. The results showed that while a well-densified microstructure with small grain size (~1 μm) and near zero porosity could be obtained by selecting a sintering schedule of 1350°C/$x$ h (48 h $< x \leqslant$ 60 h) for $CaSnO_3$ samples, very well sintered samples with relatively larger grains (3–5 μm) and minimal porosity could also be obtained by sintering at 1600°C for 2 h. Well-densified microstructure with small grain size and zero or near zero porosity could be obtained by a sintering schedule of 1350°C/$x$ h (12 h $< x \leqslant$ 24 h) in $SrSnO_3$ samples. Sintering of $BaSnO_3$ proved to be the most difficult. The $BaSnO_3$ samples could only be densified to the desired level by soaking the powder compacts for 2 h at 1600°C. The "sugar cube" features were replaced by the spherical grains (average size 1–2 μm). © 2000 Elsevier Science Ltd and Techna S.r.l. All rights reserved.

*Keywords:* Alkaline-earth metal metastannates; A. Sintering; B. Microstructure

## 1. Introduction

The alkaline-earth metastannates having the general chemical formula $MSnO_3$ (M = Ca, Sr and Ba) crystallize in simple cubic perovskite structures. They have been projected as potential electronic ceramics (thermally stable capacitors, humidity and carbon dioxide sensors, etc.) [1–6]. Recently, a number of investigations related to the synthesis of these compounds by solid-state reaction (SSR) techniques have been reported [7–10]. However, none of these reports address the important issue of correlating the synthesis and processing parameters to the microstructural aspects in the resulting bodies. This aspect is important since, in order to make a capacitor component out of $MSnO_3$, the material is required to be essentially 'pore-free', since pores would act as sink to the electrical charge carriers and would be the source of poor grain-to-grain connectivity and significant dielectric loss. Furthermore, in many of these cases, electrical data have been reported on samples sintered at a single temperature and a single soak-time. Thus, in order to fill the information gaps in the reported research, a vigorous and systematic investigation on these exotic materials was initiated. A thorough study of $MSnO_3$ compounds with respect to their synthesis, processing and microstructural development has been made. In order to establish a standard methodology for mass manufacturing at low cost on a commercial scale, with identical and beneficial microstructure and reproducible electrical characteristics, different synthesis routes (solid-state, self-heat-sustained, citrate-complex precursor and sol–gel) were adopted. Evolution of microstructure which is intimately related to the envisaged properties in the ceramics, was closely and systematically followed in terms of sintering over a wide temperature-soak time (*T-t*) profile. In this paper, the synthesis of $MSnO_3$ compounds via self-heat-sustained (SHS) reaction technique and the resulting microstructural features in their sintered compacts are presented.

---

* Corresponding author at current address: Advanced Materials Research Center, SIRIM Berhad, 1, Persiaran Dato' Menteri Section 2, 40911 Shah Alam, Selangor, Malaysia. Tel.: +60-3-556-7075; fax: +60-3-556-7092.

*E-mail address:* abmajeed_azad@hotmail.com (A.-M. Azad).

PII: S0272-8842(00)00005-5

## 2. Experimental

### 2.1. Materials synthesis and characterization

Metallic tin powder (99.999%, Pi-Kem, Surrey, UK), $Ca(NO_3)_2.4H_2O$ (98%, Fluka, UK), $Sr(NO_3)_2$ (99%, BDH, Poole, UK) and $Ba(NO_3)_2$ (99.5%, Hopkins and Williams, UK) were used as the starting materials. Metallic tin powder was thoroughly mixed with $M(NO_3)_2$ (M = Ca, Sr or Ba) crystals in 1:1 molar ratio. The mixture was placed in an alumina boat and first heated slowly to and maintained at 250°C for 4 h. This was to facilitate complete melting of metallic tin (m.p. = 232°C) and its uniform dispersion under gravitational flow in the liquid state. The temperature was then raised gradually to 800°C and maintained for another 4 h to cause the reaction between molten and free flowing tin and $M(NO_3)_2$. The temperature was monitored by placing a K-type thermocouple close to the reaction zone to ascertain the occurrence of the reaction. An X-Y chart recorder connected to the thermocouple indicated the self-heat-sustained reaction by rise in temperature at the inception of reaction. The mixture was next calcined at 1100°C for 12 h. X-ray diffraction (XRD) analysis of the resulting powder at this stage revealed the presence of predominantly two-phases ($M_2SnO_4$+$MSnO_3$) in the mixture. This necessitated further heating of the mixture at 1200°C for 24 h. The entire process was carried out in static ambient air at atmospheric pressure (1 atm).

Phase identification was carried out by powder X-ray diffraction on a Scintag or Philips X-ray machine (USA) at room temperature, using monochromatic $CuK_\alpha$ radiation ($\lambda = 1.5406$ Å) in the range 10–80° (2-theta).

Subsequent to the confirmation of ‘phase’ pure $MSnO_3$ compound formation by XRD (evidenced by the presence of all the diffraction lines corresponding to the targeted compound and absence of those corresponding to other double oxides and/or the starting individual components), the calcined powder was thoroughly blended with PVA as binder, dried and homogenized. The powder was cold-pressed uniaxially at pressures not exceeding 100 MPa into cylindrical pellets having diameter 6 and 12 mm and thickness 1–2 mm. The as-pressed pellets were subjected to sintering at three different temperatures, viz., at 1200, 1350 and 1600°C, for duration ranging from 2 to 72 h in static ambient air. The choice of a rather wide temperature-time profile in this work was to arrive at the most appropriate sintering schedule which would yield a microstructure most benign for the anticipated applications of $MSnO_3$ as electronic components.

The microstructural features of the starting ‘green’ $MSnO_3$ powder as well as the sintered discs were determined by using a JEOL-6400SM scanning electron microscope (Japan). A uniform thin film of gold was evaporated on the exposed surfaces by a Polaron coating machine (UK) to avoid electrostatic charging during microscopic viewing. Elemental identification and quantification in different regions of the sintered samples were carried out by using the EDX analyzer (Link eXL, UK) attached to the above SEM machine. Owing to strong susceptibility of the compounds in the M–Sn–O systems towards moisture, the calcined powders as well as the sintered discs were always stored in humidity-free bottles containing anhydrous $CaC1_2$, unless required for XRD or microscopic examination.

## 3. Results and discussion

### 3.1. Reaction pathway for the formation of $MSnO_3$ phase

The self-propagating high-temperature synthesis or self-heat-sustained synthesis (SHS) is an attractive and viable alternative to the conventional methods of advanced materials production, which is gaining rapid popularity in the field of ceramic–matrix composites (CMCs) and metal–matrix composites (MMCs) [11]. The most attractive feature of SHS technique is the ability of highly exothermic reactions to be self-sustained and therefore, energetically efficient. The rationale behind using metallic tin in the present case, was its rather low temperature of fusion ($<\mathrm{Sn}> = \{\mathrm{Sn}\}$ 232°C $\Delta H_f = 7.056$ kJ g atom$^{-1}$) [12], affecting a homogeneous mixing and reactivity with the metal nitrate, yielding the compound under less demanding conditions than those reported hitherto. The reason we prefer to call this technique self-heat–sustained and not the self-propagating high-temperature synthesis, is that the reaction was essentially affected under ‘open’ system conditions and, that the exothermicity of the reaction between metallic tin and the alkaline-earth nitrate did not lead to a phenomenal rise in the reaction temperature — a feature typical of the original SHS procedure. In the absence of heat capacity and enthalpy data on the reaction product ($MSnO_3$), it is difficult to compute the net enthalpy change of the reaction. Nevertheless, since the technique did yield the desired product, the assumption that the fusion of tin and subsequent reaction in the initial stages must have triggered the reaction initiation and sustained its propagation, does seem to be plausible and explicable.

The compound formation via SHS was found to have initiated at 800°C. The XRD signature of the sample after calcination at 1100°C for 12 h, however, showed a mixture of peaks corresponding to M-rich phase, viz., $M_2SnO_4$ in addition to those belonging to the intended compound $MSnO_3$, beside some peaks belonging to $SnO_2$. This is shown in Fig. l(a) in the case of (1:1) Sn:$Ca(NO_3)_2$ mixture for the sake of illustration. However, the XRD pattern of the sample calcined further at

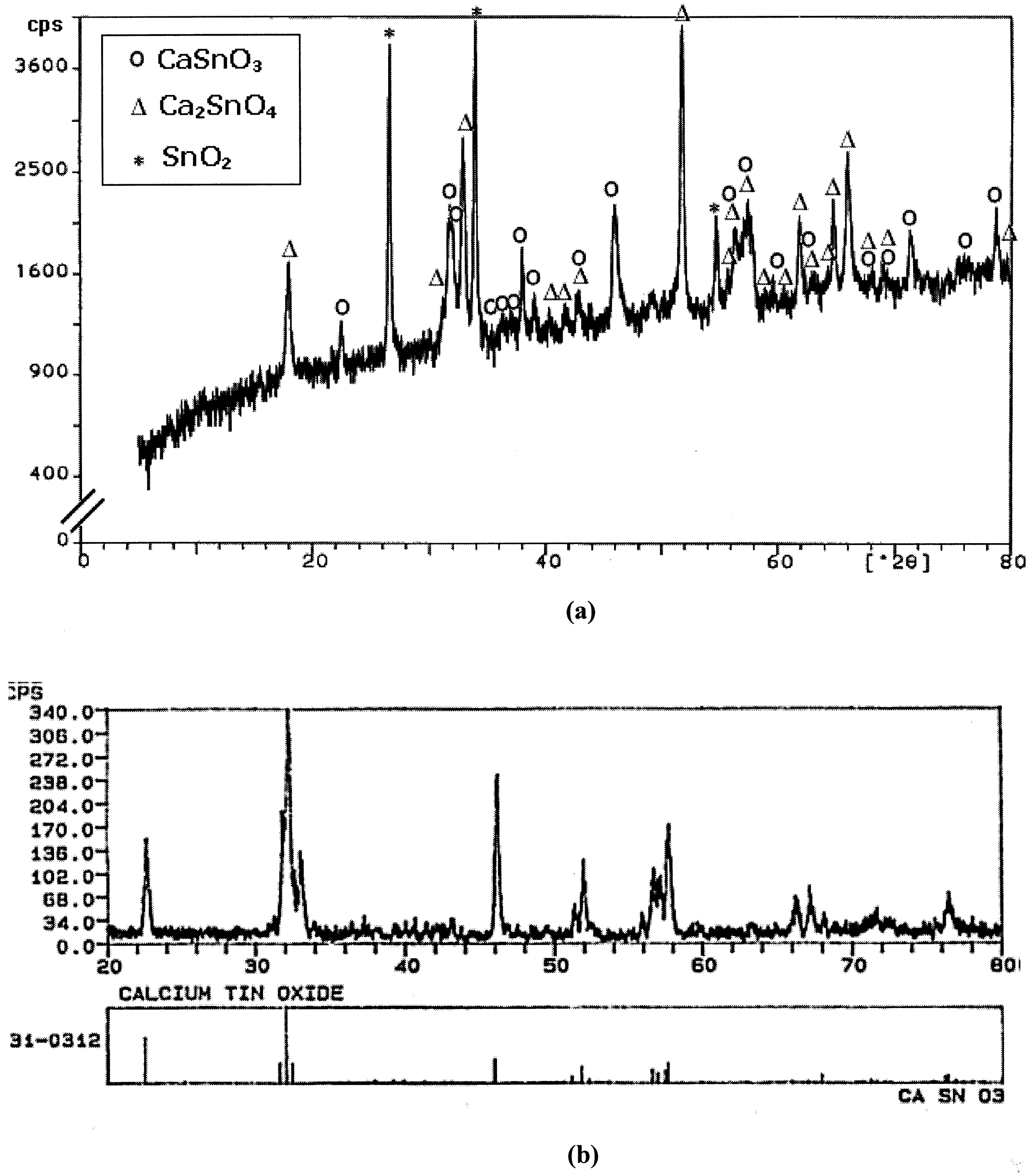

Fig. 1. Powder X-ray diffraction pattern of $CaSnO_3$ synthesized via SHS technique.

1200°C conformed to that reported for pure $MSnO_3$ and was identical to that obtained on solid-state reaction derived one [Fig. 1(b)]. The scheme of $MSnO_3$ formation by the SHS technique, therefore, seems to be via an intermediate M-rich phase, $M_2SnO_4$. It is likely that in the initial stages, molten metallic tin reacted in the following way:

$$\{Sn\} + 2 < M(NO_3)_2> \longrightarrow < M_2SNO_4 > +4(NO_2) \quad (1)$$

and

$$\{Sn\} + <M(NO_3)_2> + 1/2(O_2) \longrightarrow <MSnO_3> + 2(NO_2) \quad (2)$$

The M-rich phase subsequently reacted with more Sn or $SnO_2$ to form $MSnO_3$ as shown below:

$$< M_2SnO_4 > +\{Sn\} + (O_2) \longrightarrow 2 < MSnO_3 > \quad (3)$$

or

$$< M_2SnO_4 > + < SnO_2 > \longrightarrow 2 < MSnO_3 > \quad (4)$$

The notations < >, { } or ( ) indicate the materials in their standard solid, liquid or gaseous state, respectively.

This reaction scheme is corroborated by the XRD signature of the 1:1 molar mixture of metal nitrate and metallic tin, obtained on samples heated at 800°C/4 h

+1100°C/12 h and at 1200°C/24 h, respectively, as shown in Fig. 1 for the formation of $CaSnO_3$. The reaction pathway was found to be identical for the formation of $SrSnO_3$ and $BaSnO_3$ as well. Evolution of heat upon fusion of tin at rather low temperature is believed to have aided the above scheme of reaction pathway.

### 3.2. Microstructure in sintered $CaSnO_3$ bodies

Microstructural evolution in samples soaked at 1200°C for 12–48 h, is shown in Fig. 2(a–d). For the shorter soak-time (up to 12 h), a large number of agglomerates can be easily seen while there was not significant grain growth up to 48 h. The average grain size remained close to 1 μm, which seems to be the most salient feature of the sample synthesized by SHS technique. The densification improved systematically with corresponding decrease in porosity and intergranular connectivity was enhanced with increase in soak-time. However, one of the major limitations of SHS synthesis is the presence of relatively higher degree of porosity in the material. Nevertheless, since about 95% of this porosity is 'open' in nature, it can be eliminated during the sintering step, thereby leaving a dense and compact body. The microstructures obtained in $CaSnO_3$ discs sintered at 1350°C for 24 and 48 h are shown in Fig. 3(a,b). As can be seen clearly, there is an enhancement in density, but the remnant porosity could not be eliminated totally even after sintering at 1350°C up to 48 h. However, the small grain size (of the order of $\sim$1μm) and a narrower grain size distribution is an interesting feature in these samples. Significant yet uniform grain growth attended by further reduction in porosity can be seen in samples soaked for 2 h at 1600°C [Fig. 4(a)]. A better grain-to-grain connectivity can also be clearly observed. On increasing the soak-time from 2 to 12 h, however, the material underwent a drastic change in its microstructural constitution. The microstructure of three randomly chosen regions of the same sample is shown in

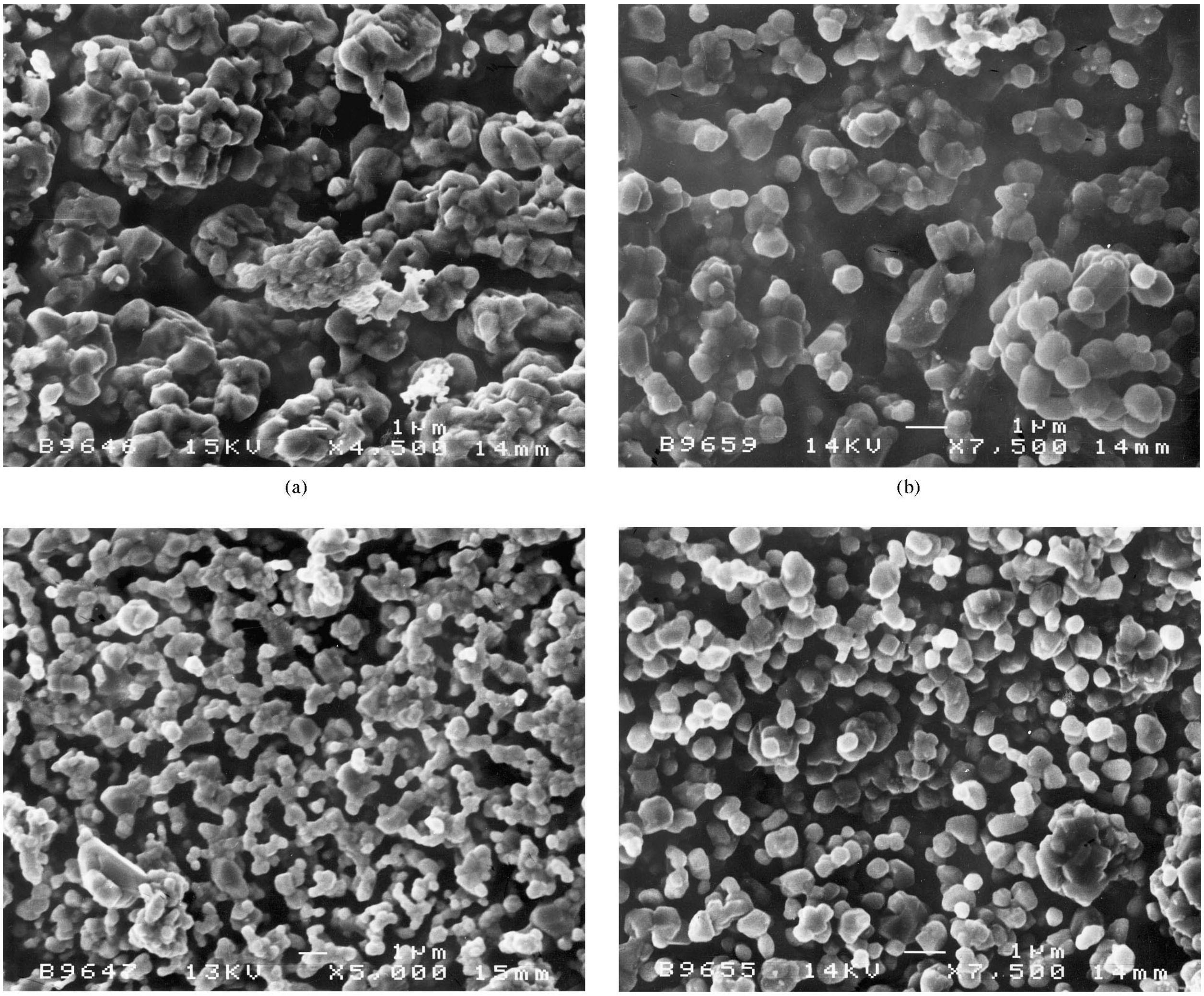

(a) (b)

(c) (d)

Fig. 2. Microstructure of $CaSnO_3$ samples sintered at 1200°C for: (a) 12, (b) 24, (c) 36 and (d) 48 h.

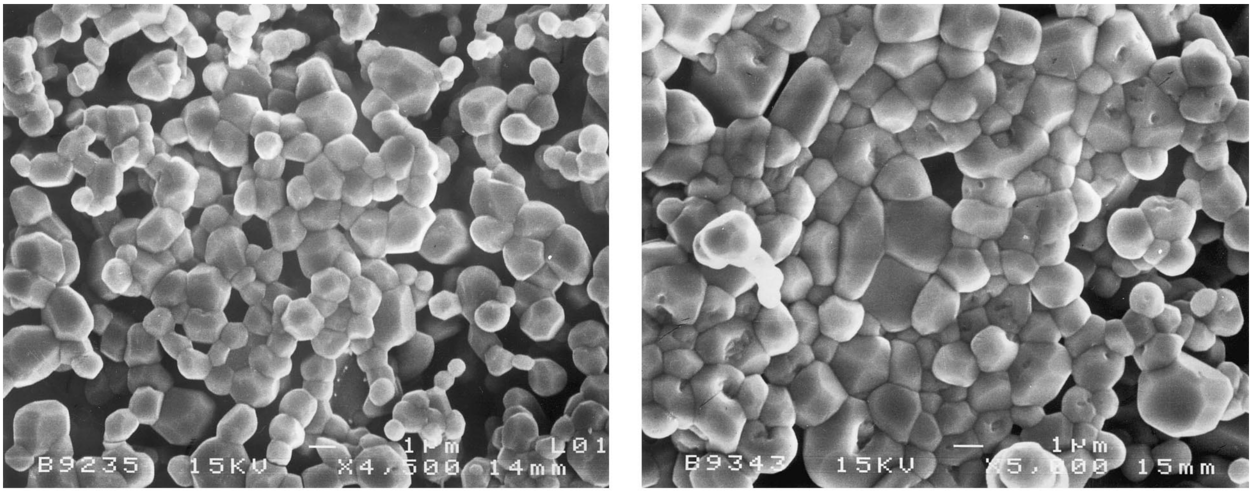

(a) (b)

Fig. 3. Microstructural evolution in $CaSnO_3$ sintered at 1350°C for: (a) 24, and (b) 48 h.

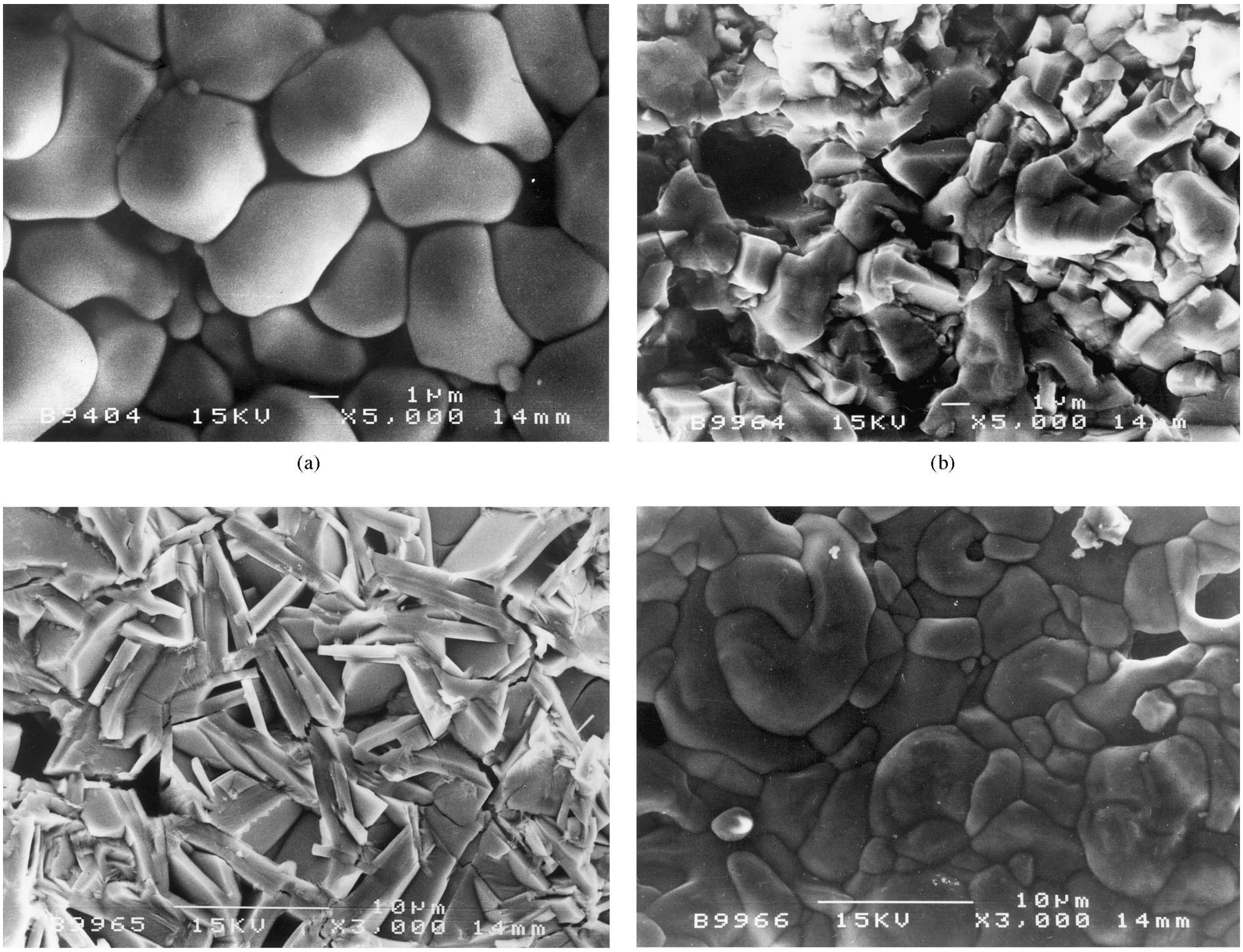

(a) (b)

(c) (d)

Fig. 4. Microstructural variation in $CaSnO_3$ sintered at 1600°C for: (a) 2 h, and (b–d) 12 h.

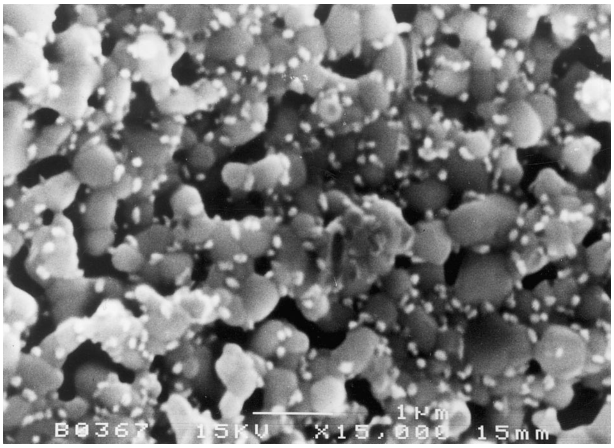

Fig. 5. Microstructural features of $SrSnO_3$ samples sintered at 1200°C for 12 h.

Fig. 4(b–d), which depicts the severity of sintering at 1600°C at longer (than 2 h) duration. Three distinct features, viz., (i) abnormal grain growth (both in shape and size), (ii) reappearance of voids in the form of very large gaping holes, and (iii) interpenetrating fractured platlets with random orientation in 3-D, can readily be seen.

### 3.3. Microstructure in sintered $SrSnO_3$ bodies

In the case of $SrSnO_3$, samples were first sintered at 1200°C for 12 h and the resulting microstructure is shown in Fig. 5, which consists of very well-connected uniformly spherical grains with a large number of open pores. The small white 'specks' distributed all across the matrix are $SrSnO_3$ formed by the tin globules of metallic tin in liquid state, concentrated mostly in the neck regions. The microstructural features on samples sintered at 1350°C for a duration ranging between 12 and 36 h, are shown in Fig. 6. The densification is seen to be near theoretical at soak-time of 12 h, accompanied by grain growth and excellent intergranular connectivity. With soak-time longer than 24 h, however, further grain growth was not noticed; the average grain size remained close to 1 μm. Thus, in the case of SHS derived $SrSnO_3$,

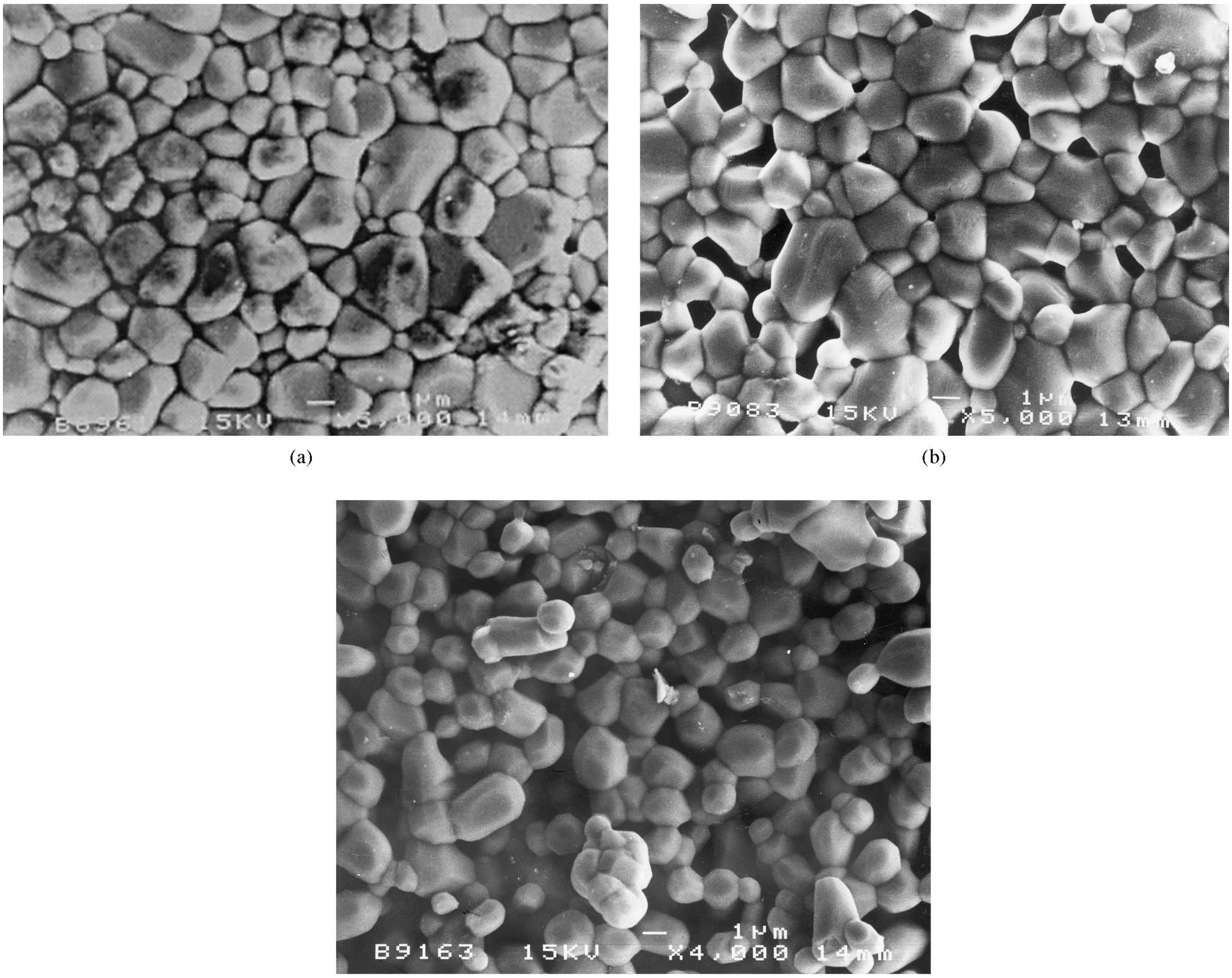

Fig. 6. Microstructural development in $SrSnO_3$ sintered at 1350°C for: (a) 12, (b) 24 and (c) 36 h.

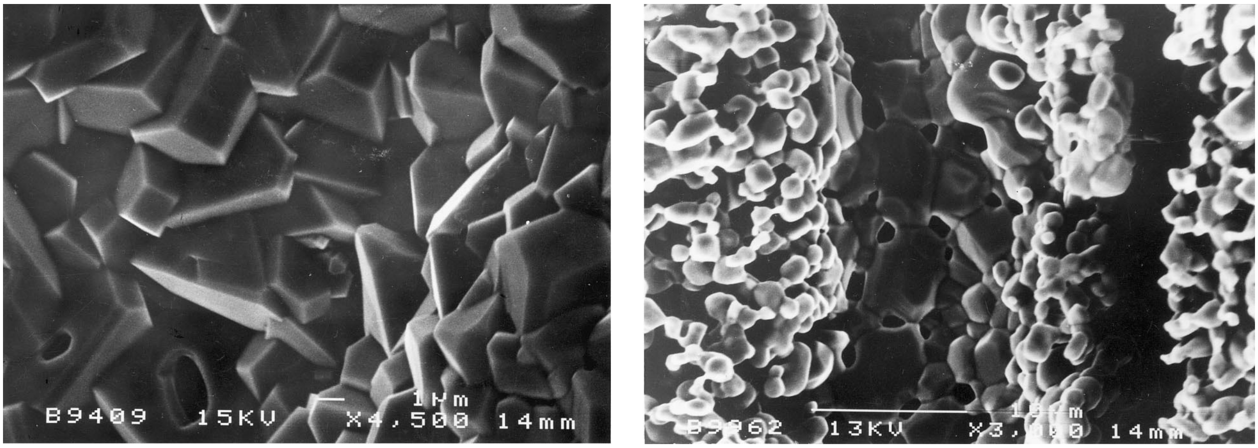

(a) (b)

Fig. 7. (a) Drastic microstructural transformation in $SrSnO_3$ samples sintered at 1600°C for 2 h and (b) Scheme of progress of variation from the normal surface layer morphology to the transformed bulk interior.

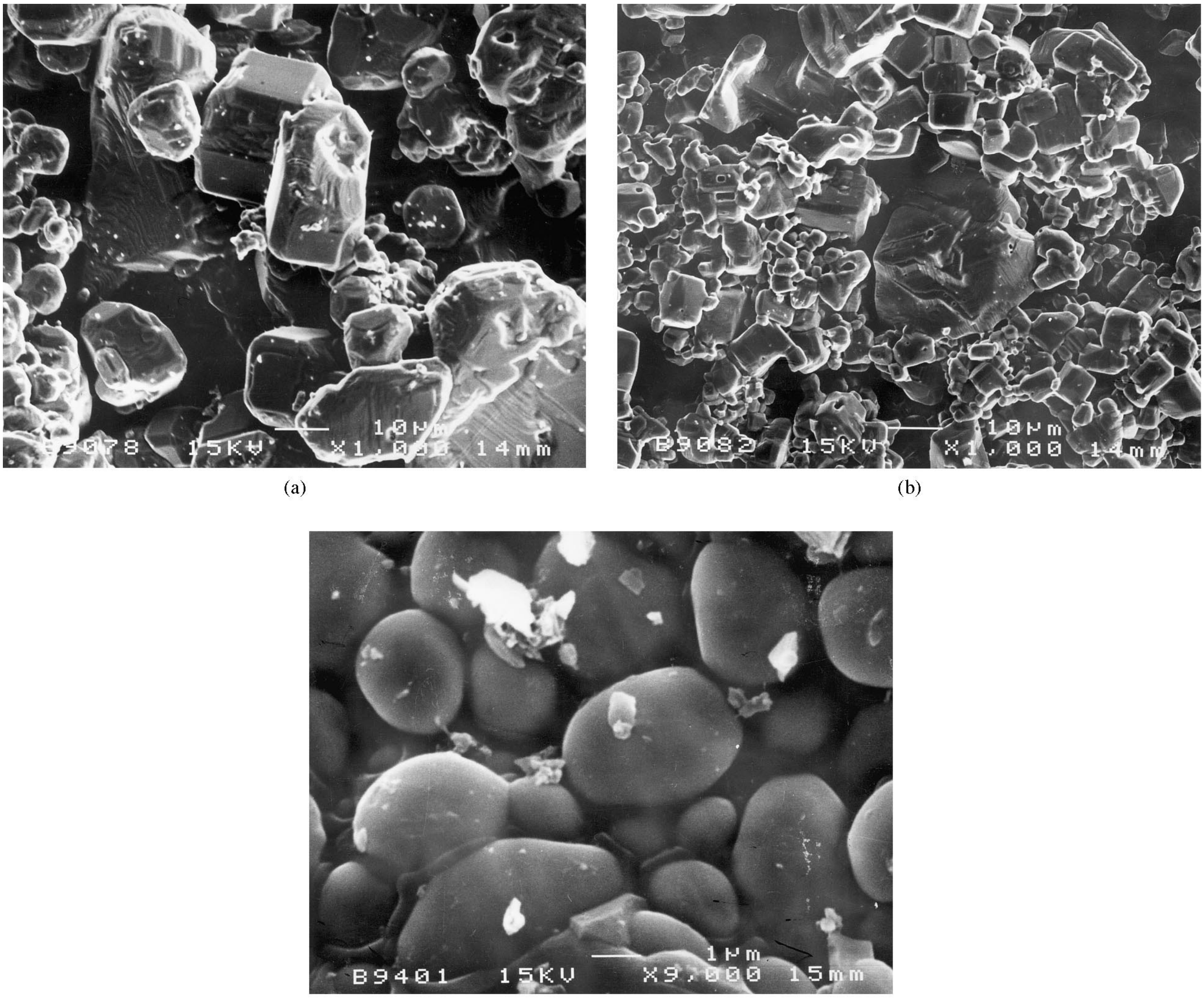

(a) (b)

(c)

Fig. 8. Microstructural evolution in SHS-derived $BaSnO_3$ sintered at 1350°C for: (a) 24, (b) 36 and (c) at 1600°C for 2 h.

sintering at 1350°C for a time period ranging between 12 and 24 h appeared to be the most benign in terms of densification and grain growth. No plausible mechanism is available at this time to explain the observed increase in porosity at soak-times exceeding 24 h. Sintering at higher temperature even for a short time, was found to be deleterious. The microstructural artifacts changed drastically in samples sintered at 1600°C for 2 h, resulting in highly oriented 3-D grains (3–5 μm in size). This is shown in Fig. 7(a). The mechanism of such a phenomenal microstructural transformation seems to be as shown in Fig. 7(b), captured in another region of the same sample. The initial well-connected small and nearly spherical grains (on the surface) are seen merged under intense heat effect at 1600°C, to form a growing angular matrix (second layer); this eventually led to the formation of fully grown and well-connected crystallites [bottom layer; same as in Fig. 7(a)].

### 3.4. *Microstructure in sintered $BaSnO_3$ bodies*

In the case of $BaSnO_3$, sintering began at 1350°C and the resulting microstructure after 24 and 36 h soak-time is shown in Fig. 8. The “sugar cube”-shaped granular features in this case are almost identical to those observed in the case of solid-state derived samples [13], albeit with much larger grain size distribution. The average size ranged from 1 to 20 μm in some overgrown grains. With increase in soak-time there was a noticeable reduction in porosity with the grain size distribution still remaining broad.

The barium stannate compacts underwent drastic morphological and structural changes subsequent to heating at 1600°C for 2 h [Fig. 8(c)]. The resulting features included: highly densified material with near zero porosity, proper grain orientation and. good intergranular connectivity. The “sugar cube” features have been replaced by the spherical grain (average size 1–2 μm).

## 4. Conclusion

A novel reaction technique (SHS) of material synthesis has been described for $MSnO_3$ compounds. The evolution of microstructure in the dense bodies as a function of sintering temperature and soak-time has been systematically followed and a correlation between processing and microstructure has been established. As a result of this, the following conclusions could be drawn.

In the case of $CaSnO_3$, well-densified microstructure with small grain size (~1 μm) and zero or near zero porosity can be obtained by choosing a sintering schedule of $1350°C/x$ h ($48 \text{ h} < x \leqslant 60$ h); very well sintered samples with relatively larger grains and minimal porosity could also be obtained upon sintering at 1600°C for a short time (2 h). In the case of $SrSnO_3$, dense compacts with small grain size and zero or near zero porosity could be obtained by sintering at 1350°C for a time period ranging between 12 and 24 h. Longer soaking at this temperature, would lead to well-connected small crystallites and open channel pores. Sintering at 1600°C even for a short time (2 h) is not at all beneficial to make a dense body containing a typical ceramic microstructure. $BaSnO_3$ samples could only be densified to the desired level by sintering the powder compacts at 1600°C for 2 h, with benign microstructural features, typical of ceramics. A comparison of microstructural evolution in $BaSnO_3$ with that in $CaSnO_3$ and $SrSnO_3$ shows a systematic trend in the gradual transition of sintering conditions, as one goes from calcium to strontium to barium. This trend can be explained in terms of the increasing ionic size (from 99 pm for $Ca^{2+}$ to 112 pm for $Sr^{2+}$ to 134 pm for $Ba^{2+}$). This difference in ionic size affects the solid-state diffusion kinetics in the corresponding ceramic- an important criterion for sintering via diffusion. A smaller ion such as $Ca^{2+}$ can diffuse faster than $Ba^{2+}$. Hence, the sintering in $CaSnO_3$ is favored and accomplished at relatively lower temperature (1200°C up to 48 h for SSR derived samples [14]). Opposite is the case with $BaSnO_3$, where a relatively high temperature (1600°C) is effective to result in near theoretical, pore-free microstructure. In addition, these stannates are line compounds with no non-stoichiometry with respect to either metal or oxygen. This is an important factor, which otherwise contributes to the sintering via cationic or anionic defect formation.

## References

[1] B. Jaffe, W.R. Cook Jr., H. Jaffe, Piezoelectric Ceramics, Academic Press, New York, 1971.
[2] A.J. Moulson, J.M. Herbert, Electroceramics: Materials, Processing, Applications, Chapman and Hall, New York, 1990.
[3] R. Buchanan, Ceramic Materials for Electronics, Marcel Dekker, New York, 1986.
[4] P.T. Moseley, A.M. Stoneham, D.E. Williams, in: P.T. Moseley, J.O.W. Norris, D.E. Williams (Eds.), Techniques and Mechanisms in Gas Sensing, Adam Hilger, Bristol, 1991, Chapter 4.
[5] Y. Shimizu, M. Shimabukuru, H. Arai, T. Seiyama, J. Electrochem. Soc. 136 (1989) 1206.
[6] U. Lumpe, J. Gerblinger, H. Meixner, Sensors and Actuators B 26-27 (1995) 97.
[7] M.G. Smith, J.B. Goodenough, A. Manthiram, R.D. Taylor, W. Kimball, C.W. Kimball, J. Solid State Chem. 98 (1992) 181.
[8] O. Parkash, K.D. Mandal, C.C. Christopher, M.S. Sastry, D. Kumar, J. Mater. Sci. Lett. 13 (1994) 1616.
[9] K.D. Mandal, M.S. Sastry, O. Parkash, J. Mater. Sci. Lett. 14 (1995) 1412.
[10] S. Upadhyay, O. Parkash, D. Kumar, J. Mater. Sci. Lett. 16 (1997) 1330.
[11] H.C. Yi, J.J. Moore, J. Mater. Sci. 25 (1990) 1159.
[12] O. Kubaschewski, C.B. Alcock, Metallurgical Thermochemistry, 5th ed., Pergamon Press, Oxford, 1979.
[13] A.-M. Azad, N.C. Hon, J. Alloys and Comp. 270 (1998) 95.
[14] A.-M. Azad, L.L.W. Shyan, P.T. Yen, J. Alloys and Comp. 282 (1999) 104.